Tornado Warning Guidance based on an Analysis of MDA/TDA/NSE Data

Caren Marzban

Abstract

The aim of this report is to offer guidance for tornado warning based on a statistical analysis of numerous variables from MDA and TDA, including some Near Storm Environmental (NSE) variables. Mention Orthogonolity .

1 Introduction

Given an algorithm involving some set of attributes for predicting some phenomenon, one is often interested in identifying the subset of the best predictors. That goal has been extensively discussed in Marzban et al. (1999) wherein it is shown that the very question is ill-defined. There it is argued that the notion of best predictors is better approached in a bivariate sense wherein the predictive strength of any predictor is assessed independently of all other variables. In the case at hand where MDA and TDA derived variables are assessed for tornado prediction, the relation between each variable and ground truth will be examined individually, without reference to any other variable.

2 Method

Two data sets spanning 83 storm days are examined: circulations detected by MDA and circulations detected by TDA. Circulations detected by both MDA and TDA, jointly, are included in each of the two data sets. Tornados (nontornados) are generally referred to as 1's (0's). The a-priori (i.e., climatological) probability of tornadoes will also be addressed, and for that analysis the effect of a BWER detection is also examined.

The number of circulations, N, and the a-priori tornado probability, $p_1 = N_1/N$, where N_1 is the number of tornadic circulations, is given in Table 1. MDA' stands for MDA circulations with rank≥ 5, and TDA' stands for TDA circulations with low-level gate-to-gate velocity difference ≥ 25, maximum gata-to-gate velocity difference ≥ 36, base $< 600m$ (or detection on the first elevation), and depth $\geq 1500m$.

Range	overall		0-50km		51km-100km		101-150km		$\geq$ 151km	
	N	p_1	N	p_1	N	p_1	N	p_1	N	p_1
MDA	51641	0.05	10453	0.04	16980	0.06	13697	0.05	10511	0.04
TDA	20712	0.09	4853	0.07	9867	0.09	5992	0.09	—	—
MDA'+TDA'	2840	0.34	638	0.34	1241	0.38	959	0.30	2	0.50†
BWER	10608	0.12	3376	0.09	4585	0.13	2270	0.15	377	0.17
MDA+BWER	6287	0.15	2036	0.11	2476	0.17	1398	0.18	377	0.17
TDA+BWER	5619	0.15	1660	0.12	2703	0.15	1250	0.18	—	—
MDA'+TDA'+BWER	1298	0.38	326	0.37	595	0.41	376	0.33	1	0.00†
MDA'	7899	0.19	1539	0.19	2223	0.27	2064	0.19	2073	0.13
TDA'	2494	0.29	504	0.22	1097	0.32	893	0.28	—	—
MDA'+BWER	2137	0.31	550	0.30	849	0.36	559	0.28	179	0.25
TDA'+BWER	789	0.45	133	0.53	366	0.51	290	0.34	—	—

Table 1: The sample size and the prior (climatological) probability of tornado for different range intervals. The values marked with a †are highly unreliable because of the small corresponding sample sizes; all three circulations have a range of 152km. Note that TDA's range does not exceed 150km.

Evidently, Table 1 implies that TDA circulations meeting the restrictions that define TDA' (above) accompanied by a BWER are highly likley (45%) to be tornadic. A circulation detected by MDA and TDA has a 34% probability of being tornadic, and that probability is raised to 38% if the circulation is accompanied with a BWER.

It is interesting to assess the range-dependence of these prior (climatological) probabilities. Four different range intervals are considered and Table 1 displays that information as well. It can be seen that with a few exceptions the overall probabilities are mostly constant, independent of range. The exceptions are MDA', TDA', MDA'+BWER, and TDA'+BWER, for which there may be a change as large as 10% in the prior probabilities.

It may be worth mentioning that the sample sizes for MDA are those after all zero-rank circulations have been removed. Specifically, the MDA sample size prior to the exclusion of the zero-rank cases is 168625. There are several reasons why these cases are excluded from the analysis, but the most important reason is that WDSS/WATADS does not display MDA detections with zero strength rank.

In addition to rank-zero circulations, both the missing values and outliers are excluded. Although the former are easily identified, the isolation of the latter calls for human intervention. In particular, the class-conditional probability density function of every variable is visually inspected, and the outliers identified and excluded.

Several methods are employed to assess the predictive strength of every variable. First, the linear correlation coefficient, r, between a variable and ground truth is computed. This provides a measure of the linear association between every variable and ground truth.

Second, a threshold is placed on every variable, and varied from the minimum to the maximum value of the variable. At each value of the threshold, a contingency table is formed,

$$\begin{pmatrix} c_{00} & c_{01} \\ c_{10} & c_{11} \end{pmatrix} = \begin{pmatrix} \text{\# of 0's predicted as 0} & \text{\# of 0's predicted as 1} \\ \text{\# of 1's predicted as 0} & \text{\# of 1's predicted as 1} \end{pmatrix},$$
$$= \begin{pmatrix} . & \text{false alarms} \\ \text{misses} & \text{hits} \end{pmatrix}.$$

from which the following measures are computed:

$$\begin{aligned} \text{Probability of Detection (POD)} &= c_{11}/N_1, \\ \text{False Alarm Rate (FAR)} &= \frac{c_{01}}{c_{01}+c_{11}}, \\ \text{False Alarm Ratio (FA)} &= c_{01}/N_0, \\ \text{Heidke Skill Score(HSS)} &= \frac{2(c_{00}c_{11} - c_{01}c_{10})}{(c_{01}+c_{11})N_0 + (c_{00}+c_{11})N_1}. \end{aligned}$$

The maximum value of HSS allows for the assignment of a predictive strength to every variable. The maximum value of HSS, as a function of the threshold placed on every variable, is a measure of the predictive strength of that variable.

Finally, it is possible to assign a predictive strength to every variable without reference to a specific value of the threshold. This is in contrast to the previous method where the maximum of HSS (i.e., the predictive strength of the variable) is associated with a specific value of the threshold. Plotting POD vs. FA as the threshold varies over its full range produces a curve referred to as a ROC curve (Marzban 2000). For random forecasts the curve is a diagonal line of slope one. For skillful forecasts, the curve extends from the origin to the point (1,1), but it slides above the diagonal line. The area under the curve is a measure of the predictive strength of the variable, regardless of any specific value of the threshold. Since the area under the ROC curve of a random classifier is 0.5, it is convenient to gauge the predictive strength of a variable as $|\text{area} - 0.5|$. We shall refer to this quantity simply as ROC. As such, higher values of ROC signify higher predictive strength, and ROC=0 suggests no predictive strength at all. Although, ROC, as a scalar measure allows for the assignment of predictive strength, the ROC curve (as a 2-dimensional entity) conveys more information. For this reason, after the best predictors are identified based on ROC, we shall revert to the ROC curve itself for a more complete expression of predictive strength.

In addition to the ROC curve, there are two other 2-dimensional quantities that reflect the predictive strength of a variable. These are the class-conditional liklihoods, and the posterior probability of tornado occurrence. Both are defined in Marzban (1998). Briefly, the former are simply the probability density functions for tornadic and nontornadic circulations, seperately. These are the probability of obtaining some value of the variable, given that the corresponding circulation is tornadic or nontornadic. The separation between these two probabilities gauges the extent to which the corresponding variable can discriminate between tornadic and nontornadic circulations. The second 2-dimensional quantity is the probability of obtaining a tornadic circulation, given a

MDA	(40,39), (55,120), (54,57), (106,127), (101,130)
TDA	(20,21), (36,101), (35,38), (82,111), (87,108), (79,111)

Table 2: Equivalent pairs of variables for MDA and TDA.

specific value of the variable. This posterior probability, $P_1(x)$, is computed from the liklelihoods using Bayes' Theorem. Given the impracticality of managing hundreds of diagrams displaying likelihoods and posteriors, these diagrams will be displayed only for the best predictors selected according to the previous methods.

Another important question is that of the range-dependence of the best predictors. Specifically, the question is whether or not the list of best predictors will vary with range, and whether or not there is a significant change in the value of the threshold that maximizes performance. Both of these questions will be answered.

Among all of the hundreds of variables that are examined, there are a handfull whose "interaction" is also of interest. Scatterplots will be employed to address this issue.

Scatterplots will also be employed to find a proxy for low-altitdue mesocyclone strength. In other words, scatterplots of low-level rotational velocity and various NSE variables will be examined but only for circulations whose base fall in the range 0.5km to 1.5km.

Finally, in order to explore the dependence of the results on different storm types, many of the above analyses will be repeated for four different storm types. The four types are: Isolated supercells, mini supercells, Squall Line Tornadoes, and Tropical Cyclone Tornadoes.

3 Results

Appendix A lists all of the variables and the numerical labels by which they will be referenced throughout this report. There are generally two groups of variables, radar variables, and NSE variables. The latter are labeled 31-154 for MDA, and 12-135 for TDA.

The linear correlation between the variables can shed some light on their possible (statistical) equivalence. In other words, variables that are highly correlated for both tornadic and nontornadic circulations may be considered statistically equivalent. Pairs of variables whose linear correlation exceeds 0.9 are listed in Appendix B. It can be seen that many attributes are not independent and may be considered (statistically) equivalent. (The pairs 131 and 83 in MDA, and 112 and 64 in TDA, are identical variables which were accidentally assigned two different labels.) Some of the outstanding equivalent pairs are given in Table 2.

In passing, note that according to Table 1, a TDA detection is nearly twice as likely to be tornadic than an MDA detection.

	Criterion	Radar Variables	NSE Variables
MDA	ROC	20, 8, 29, 25, 27, 9, 15	120, 115, 56, 55
	HSS	20, 29, 21, 25, 4, 8, 27	115, 56
	r	20, 29, 8, 25, 21	56, 120
TDA	ROC	1, 4, 3, 9	96, 134, 85
	HSS	3, 4, 1, 2	96, 72
	r	4, 3, 1	96, 85

Table 3: The outstanding predictors for MDA and TDA according to three different crteria. Underlined variables have equal predictive strengths.

The predictive strength of each variable according to the three methods is displayed in Figure 1 (for MDA) and Figure 2 (for TDA). The error bars are standard errors.

It can be seen that the best predictors are among the radar variables, although some of the NSE variables have predictive strengths comparable to some of the radar variables. The outstanding predictors, in descending order, are given in Table 3 (underlined variables have equal predictive strengths):

In other words, regardless of the measure of performance, x20 (Meso Strength Index) is the best predictor for MDA, followed closely by x8 (Meso low-level rotational velocity) and x29 (Meso Integrated Rotational Strength (IRS) index). The top predictors for TDA are x3 (TVS low-level gate-to-gate velocity difference) or x4 (TVS maximum gate-to-gate velocity difference), depending on whether HSS or r is employed as the measure of peformance, and x1 (TVS base).

Among the NSE variables, the choice of the best predictor for MDA depends on the choice of the measure of performnce. Therefore, in no particular order, the best MDA NSE predictors are x120 (Maximum Bouyancy), x115 (55% UNEL, corresponding to 0-6 km, shear magnitude), and x56 (grid-relative average surface pressure). The best TDA NSE predictor is unambiguously x96 (average omega (vertical velocity; microbars/sec) in the 850-500mb layer).

Figures 3, and 4 show some multi-dimensional measures of performance for the best predictors of MDA and TDA, respectively. The left diagrams show the liklihoods for nontornadoes (black), tornadoes (red), and the posterior probability of tornado (green) as a function of three of the best predictors. The right diagrams display how HSS (black), POD (red) and FAR (green) vary as a function of the threshold placed on each of the three best predictors. The insets show the ROC curves; again, a curve stretching to the upper left indicates better performance.

The utility of the left figures is in identifying the threshold at which performance is maximized. For x20, x9, and x29 in MDA, the critical threshold are 4000, 20, and 3500, respectively. The value

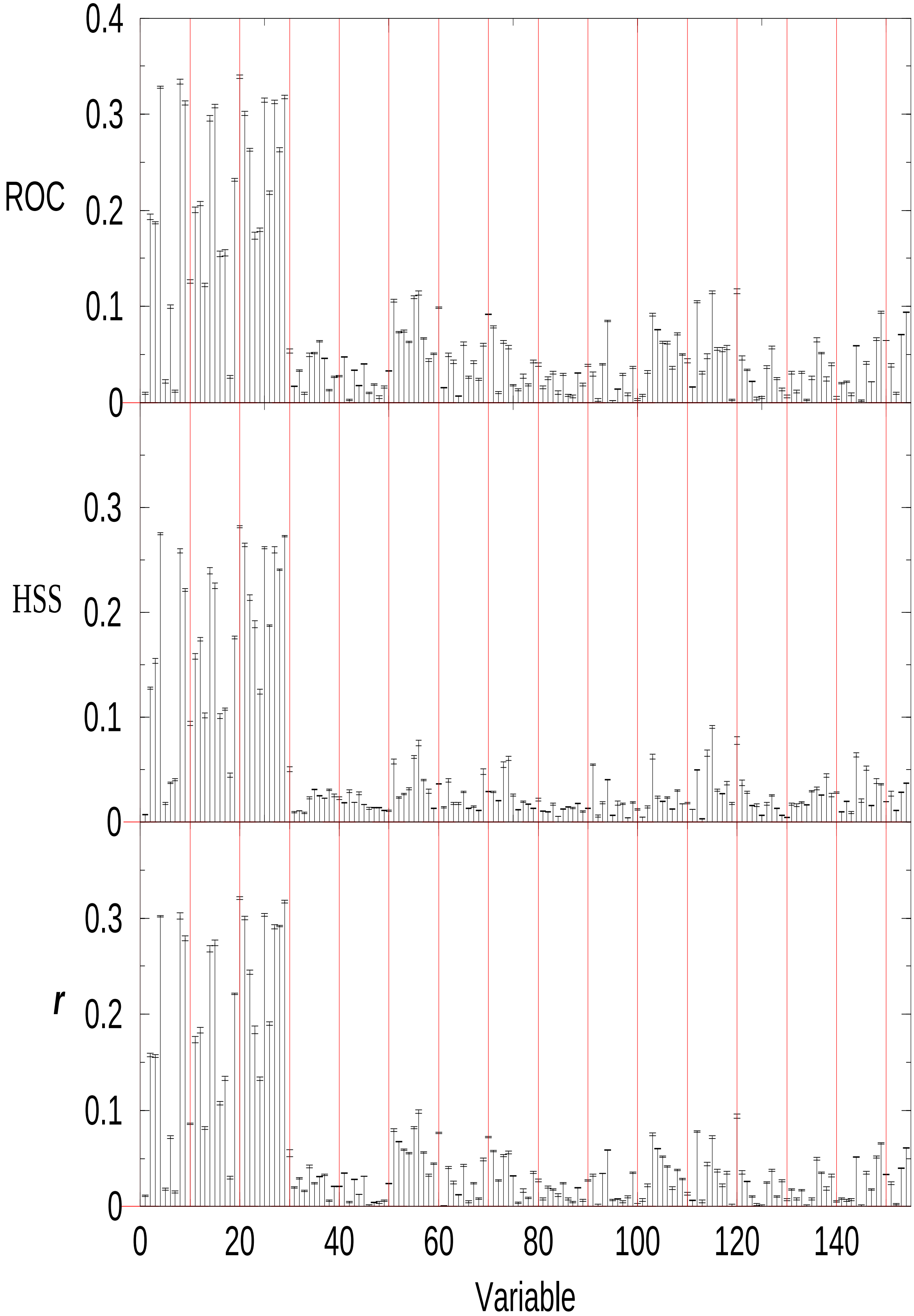

Figure 1: Predictive stength of MDA variables according to three measures of performance.

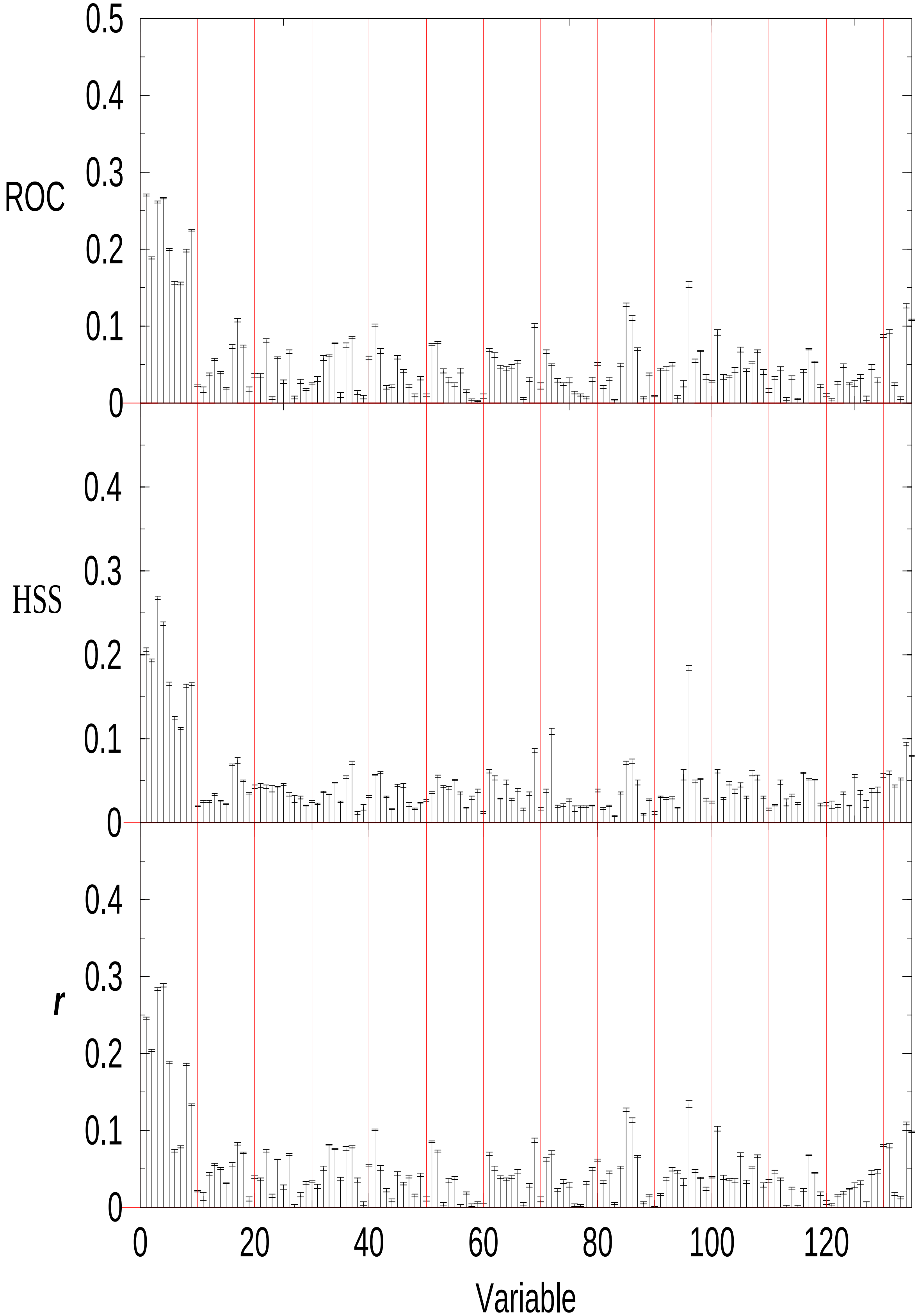

Figure 2: Predictive stength of TDA variables according to three measures of performance.

of HSS at these critical thresholds is nearly 30%, with POD=45% and FAR=75%.

As for TDA best predictors, x3, x4, and x1, the respective thresholds are 30, 40 and 1500, with HSS=20%-25%, POD=40%-50% and FAR=70%-80%.

One question that arises is whether the critical value of the threshold that maximizes HSS actually depends on the range of the circulation from the Radar. To address this question, the data were partitioned into 50km intervals, and the above analysis was repeated. Figures 5 show HSS as as a function of the threshold, for several different range intervals. Four range intervals are considered: 0-50km (black), 51km-100km (red), 101-150km (green), and $\geq$ 151km (blue). For TDA, only the first three intervals exist. It can be seen that for the best MDA predictors, there is very little change in the critical threshold of HSS for different range intervals. However, from the height of the HSS curves (and the ROC diagrams in the insets), it can be seen that the best performance of these variables is in the 51km-100km (red) range, and the worse performance is in the $\geq$ 150km (blue) range.

The same conclusions apply to the best TDA predictors with the exception of x1 for which there is significant dependence of the critical threshold of HSS on the range interval. For the three range intervals, the critical thresholds are 50, 150, and 200 respectively. Another significant differenc with the other best predictors is that the best performance of x1 in the first interval (0-50km (black)) is comparable to that in the second range interval (51km-100km (red)).

Figure 6 displays the "interaction" between x8 (for MDA) and x3 (for TDA) (radar variables) with some of the NSE variables. (Greg, I don't see anything here.)

As for the proxy for low-level rotational velocity, the scatterplots in Figure 6 are reproduced in Figure 7, but only for circulations whose base is restricted to the 0.5-1.5km interval. (Greg, again, I don't see anything here.)

4 Results: Specific Storm Types

In this section some of the above results are reproduced but for four different storm types.

The prior (climatological) probability of tornadoes is informative. Whereas, in general, a TDA detection is twice as likely to be tornadic than an MDA detection (Table 1), this probability actually depends on storm type (Table 4). For isolated storms a TDA detection is nearly 16 times more likely to be tornadic, with that factor reducing to nearly 2 (for mini supercells and squall lines), and 1 (for tropical storms). Note that for Tropical storms a TDA detection and an MDA detection are equally likely to be tornadic.

The list of best predictors depends not only on the measure of performance, but also on storm type. Based on the figures in Appendix C, the best predictors are tabulated in Table 5 (underlined variables have equal predictive strengths).

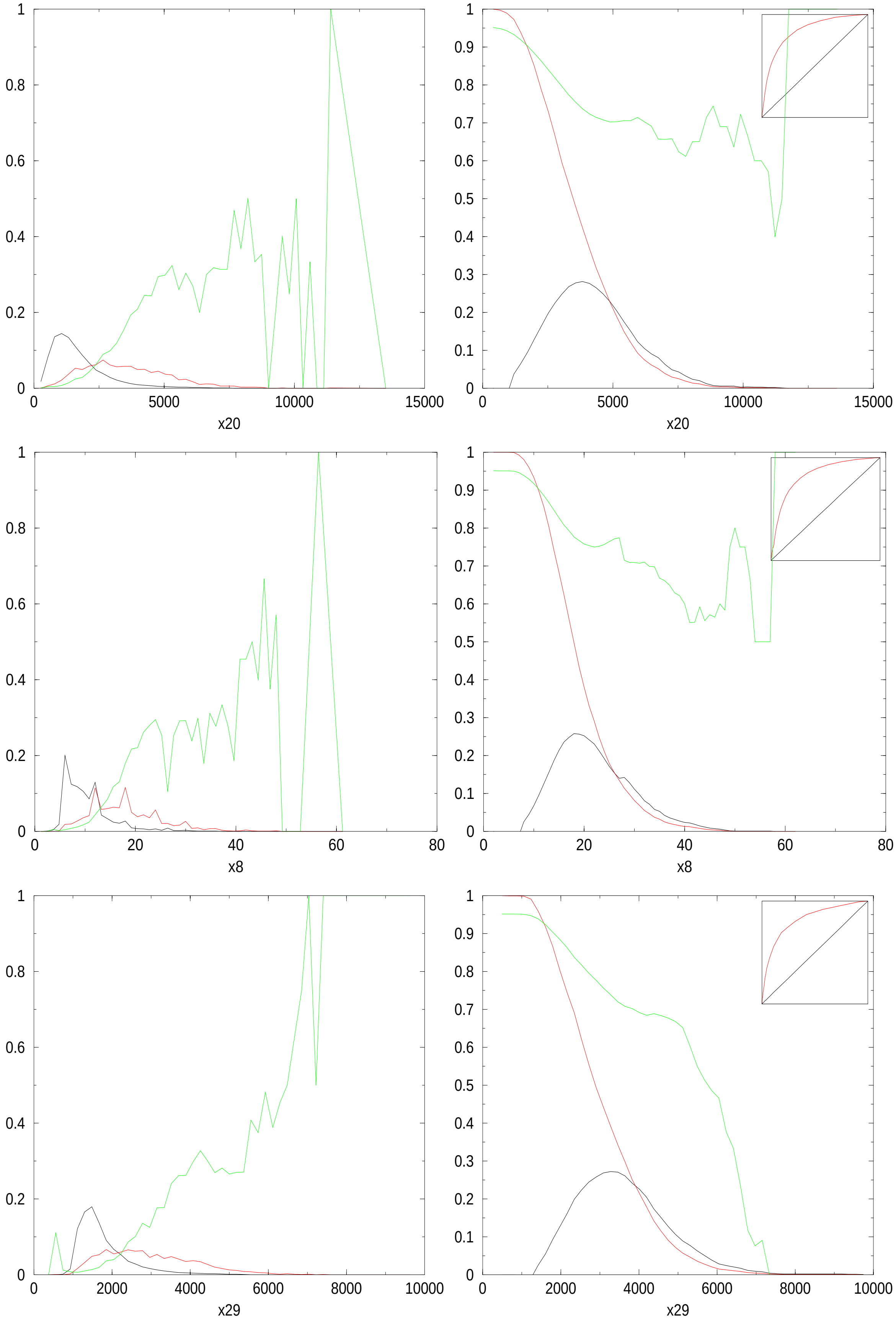

Figure 3: Left: The class-conditional distribution, and the posterior probability of tornado as a function of the MDA's best predictors. Right: HSS, POD, and FAR as a function of the threshold placed on the MDA's best predictors; the inset displays POD vs. FA, namely the ROC diagram.

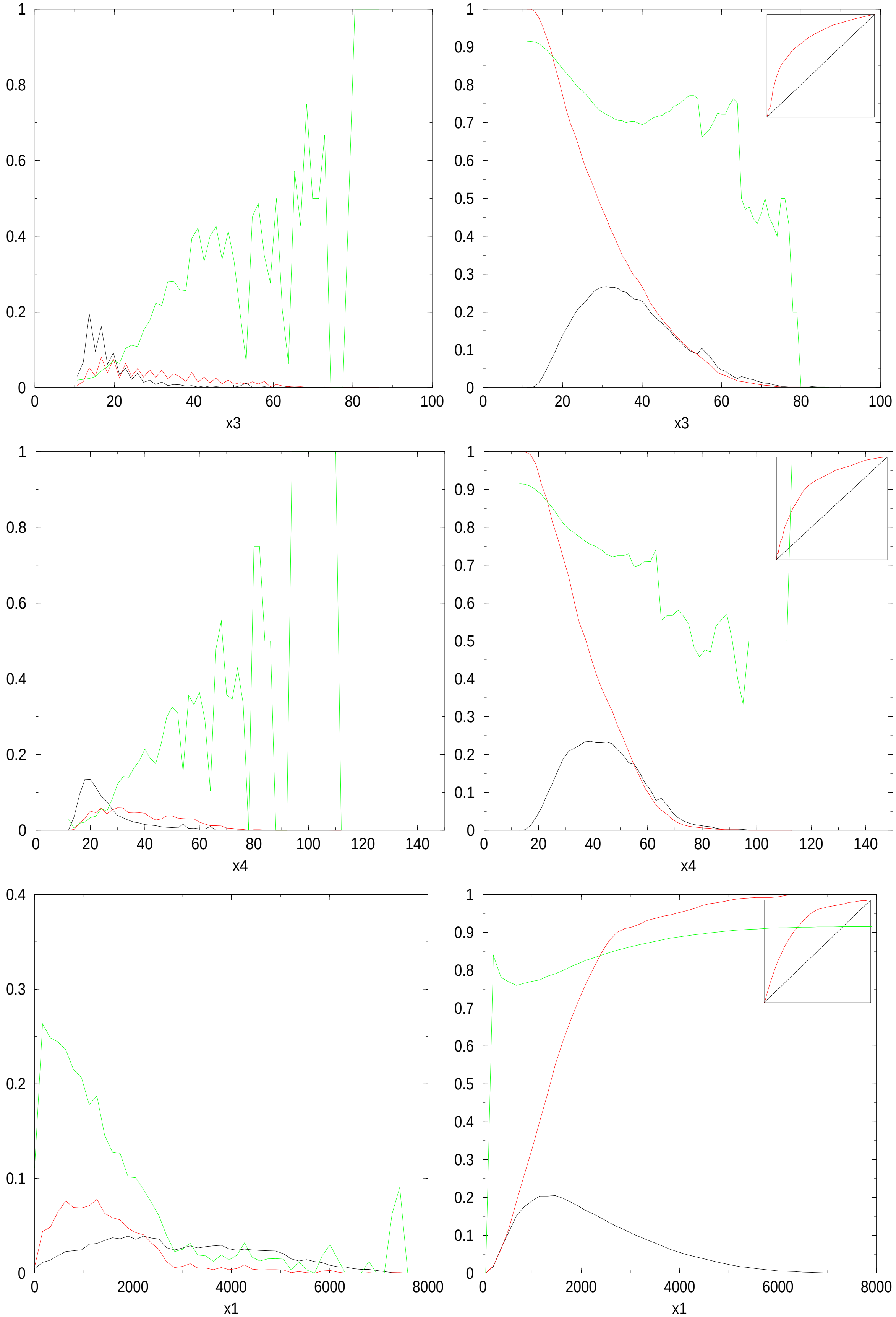

Figure 4: Left: The class-conditional distribution, and the posterior probability of tornado as a function of the TDA's best predictors. Right: HSS, POD, and FAR as a function of the threshold placed on the TDA's best predictors; the inset displays POD vs. FA, namely the ROC diagram.

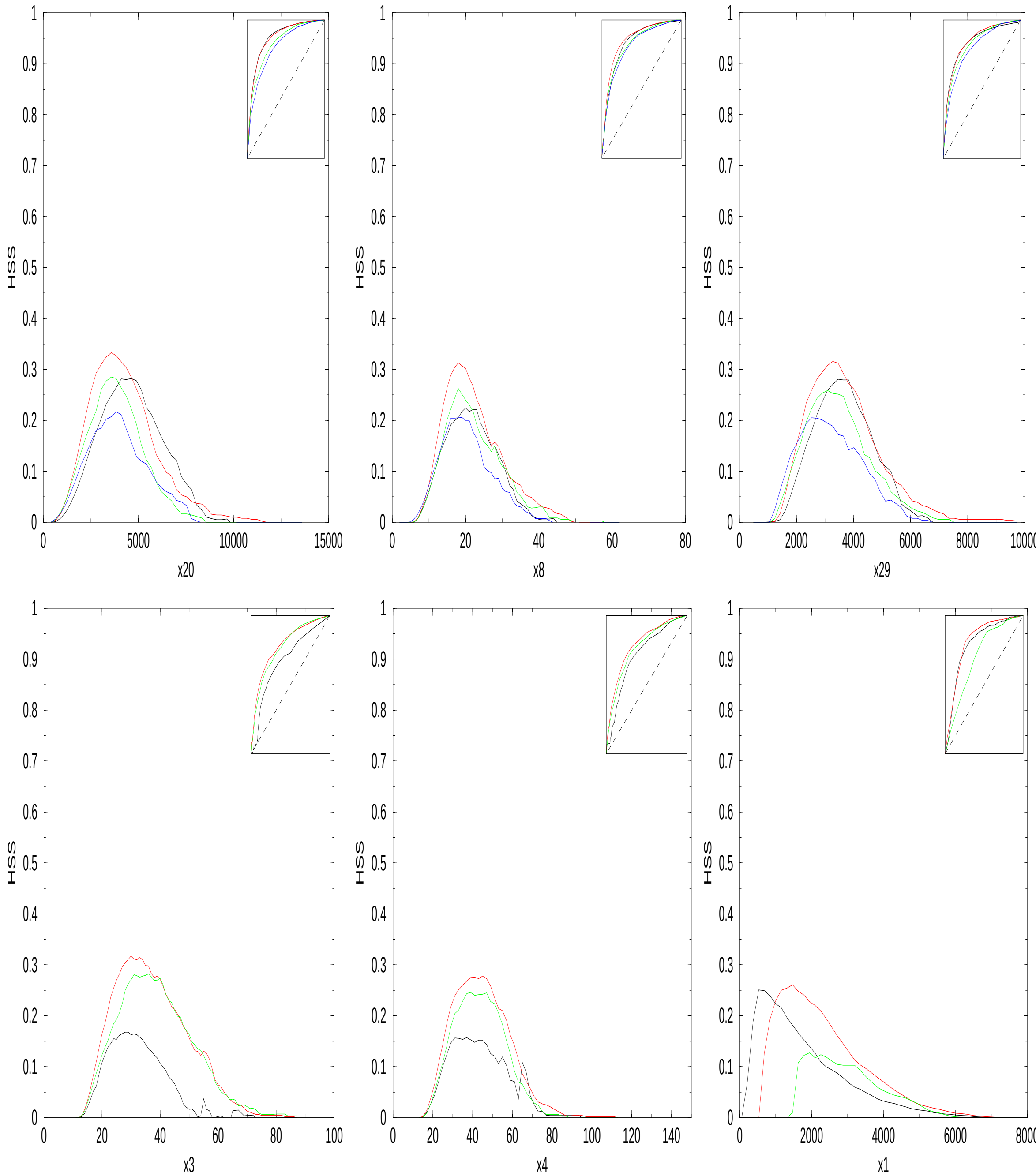

Figure 5: The range dependence of HSS as a function of the threshold placed on the top 3 predictors for MDA (top), and TDA (bottom). The insets display the ROC diagram; a curve stretched to the upper-left corner

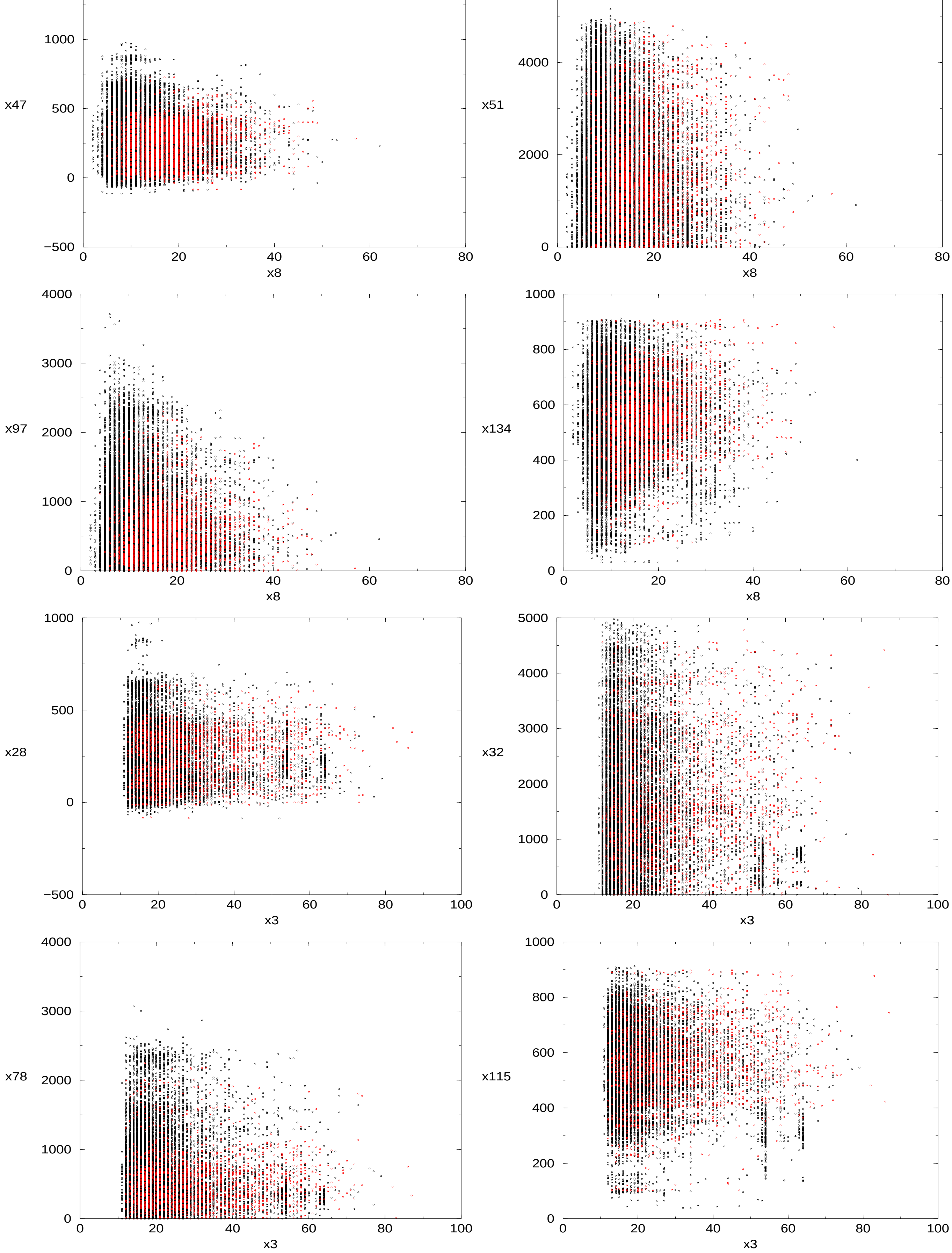

Figure 6: "Interaction" between a radar variable and some NSE variables. The black (red) circles represent nontornadic (tornadic) circulations.

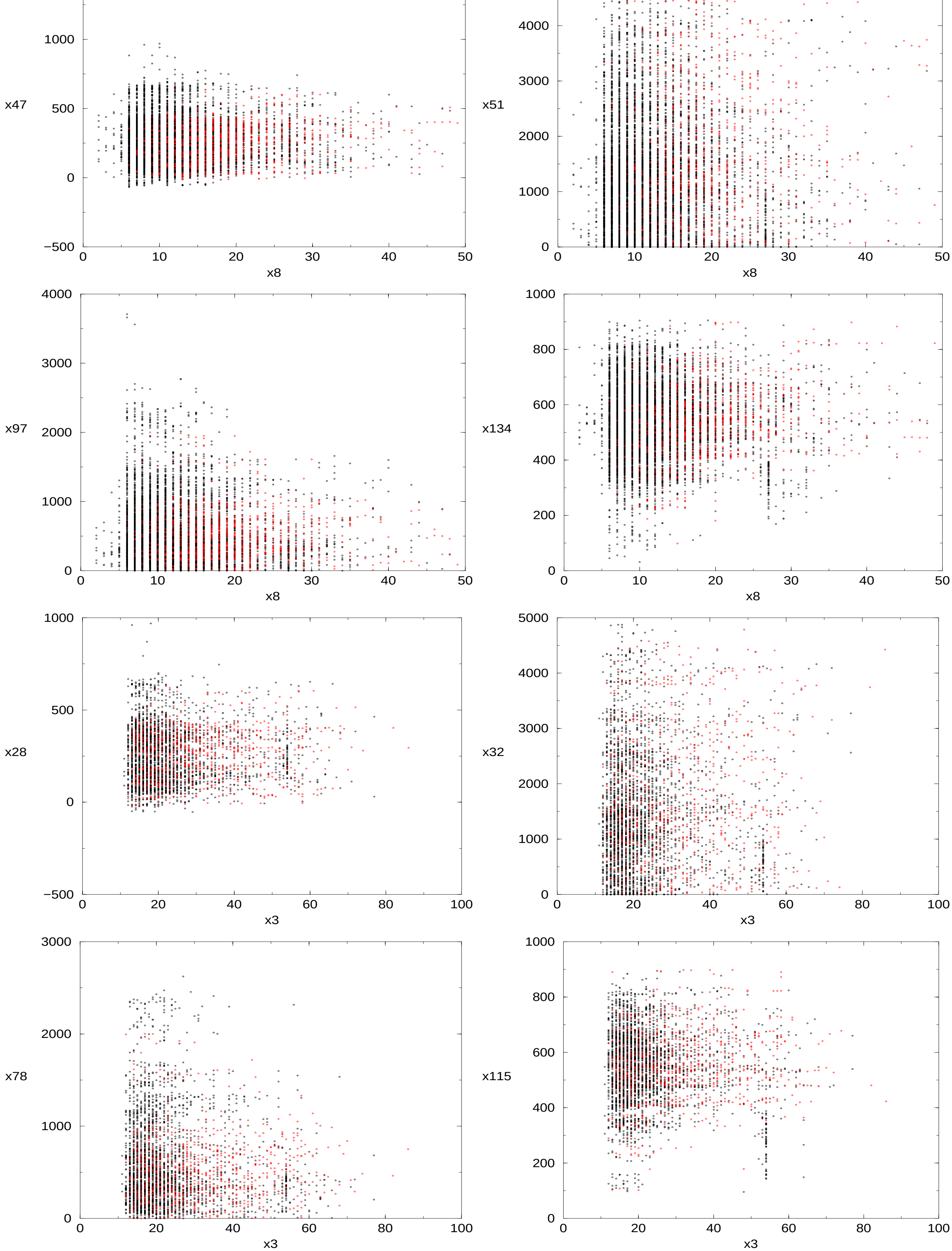

Figure 7: Low-level rotational velocity. The black (red) circles represent nontornadic (tornadic) circulations.

	Isolated		Mini supercell		Squal		Tropical	
	N	p_1	N	p_1	N	p_1	N	p_1
MDA	39871	0.06	1839	0.04	8312	0.02	1767	0.04
TDA	16719	0.10	467	0.06	2955	0.04	607	0.04
MDA'+TDA'	2474	0.36	43	0.19	283	0.22	44	0.25
BWER	9810	0.13	246	0.02	581	0.06	25	0.16
MDA+BWER	5792	0.16	178	0.03	336	0.08	22	0.18
TDA+BWER	5259	0.16	79	0.01	288	0.07	8	0.25
MDA'+TDA'+BWER	1241	0.38	11	0.00	43	0.28	5	0.40
MDA'	6272	0.23	121	0.13	825	0.11	692	0.03
TDA'	1473	0.47	14	0.29	122	0.20	56	0.03
MDA'+BWER	2029	0.32	18	0.00	89	0.21	8	0.38
TDA'+BWER	767	0.46	6	0.00	17	0.29	1	0.00

Table 4: The sample size and the prior (climatological) probability of tornado for different storm types.

		Isolated	Mini supercell	Squal	Tropical
MDA	ROC	20, 8, 4	8, 119, 121, 115	20, 8, 4, 29, 25	19, 91
	HSS	20, 29, 27	118, 115, 22	28, 25, 29	19, 91, 30
	r	20, 29, 27	8, 4	28, 20, 29	19, 91, 30
TDA	ROC	4, 3, 1	99, 102, 98, 100	1, 9, 4	22, 26, 18, 72, 24
	HSS	3, 4, 1	99, 96, 102	3, 7, 9, 80	72, 48, 18
	r	3, 4, 1	99, 102, 69, 72	3, 4, 9	72, 18, 22, 24, 26

Table 5: The outstanding predictors for different storm types.

As for what is the set of best predictors, most results are ambiguous and depend on the measure of performance. The unambiguous finds can be summarized as follows. For isolated storms, the best predictors are x20 for MDA, and x4, x3, x1 for TDA. For mini supercells, x99 is the best TDA predictor. For tropical storms x19 and x91 are the best MDA predictors, and x72 and x18 are the best TDA predictors.

5 Appendix A

This appendix lists the variables and their identifying numbers by which they are referenced in the text.

MDA

1. Meso Range (km) [0-230]
2. Meso base (m) [0-12000]
3. Meso depth (m) [0-13000]
4. Meso strength rank [0-25]
5. Meso low-level diameter (m) [0-15000]
6. Meso maximum diameter (m) [0-15000]
7. Meso height of maximum diameter (m) [0-12000]
8. Meso low-level rotational velocity (m/s) [0-65]
9. Meso maximum rotational velocity (m/s) [0-65]
10. Meso height of maximum rotational velocity (m) [0-12000]
11. Meso low-level shear (m/s/km) [0-175]
12. Meso maximum shear (m/s/km) [0-175]
13. Meso height of maximum shear (m) [0-12000]
14. Meso low-level gate-to-gate velocity difference (m/s) [0-130]
15. Meso maximum gate-to-gate velocity difference (m/s) [0-130]
16. Meso height of maximum gate-to-gate velocity difference (m) [0-12000]
17. Meso core base (m) [0-12000]
18. Meso core depth (m) [0-9000]
19. Meso age (min) [0-200]
20. Meso strength index (MSI) wghtd by avg density of intgrtd lyr [0-13000]
21. Meso strength index (MSIr) "rank" [0-25]
22. Meso relative depth (%) [0-100]
23. Meso low-level convergence (m/s) [0-70]
24. Meso mid-level convergence (m/s) [0-70]
25. Meso Vertically-integrated rotational velocity (m/s) [0-40]
26. Meso Vertically-integrated Shear (m/s/km) [0-100]
27. Meso Vertically-integrated gate-to-gate vel. diff. (m/s) [0-60]
28. Meso Integrated Rotational Strength (IRS) index (NWS method -
29. Meso Integrated Rotational Strength (IRS) index (MSI method -
30. BWER Overall Confidence (0-100%)
31. d2d(1, : actual surface pressure (mb)
32. d2d(2, : number of upper-air pressure levels lying below ground
33. d2d(3, : surface u-component (north-relative ; m/s)
34. d2d(4, : surface v-component (north-relative ; m/s)
35. d2d(5, H253: height of the 253 K temperature surface (m agl)
36. d2d(6, H273: height of the 273 K temperature surface (m agl)

37. d2d(7, UAVE: average u-component over a specified depth (north-relative)
38. d2d(8, VAVE: average v-component over a specified depth (north- relative)
39. d2d(9, : average wind speed over a specified depth (m/s)
40. d2d(10, STSP: estimated storm speed (m/s)
41. d2d(11, : u-component of estimated storm motion vector(north-relative)
42. d2d(12, : v-component of estimated storm motion vector(north-relative)
43. d2d(13, : same as 7, , except for grid-relative. See subroutine
44. d2d(14, : same as 8, , except for grid-relative
45. d2d(15, : same as 11, , except for grid-relative
46. d2d(16, : same as 12, , except for grid-relative
47. d2d(17, SRH3: estimated 0-3 km storm relative helicity
48. d2d(18, SFRH: surface relative humidity (percent)
49. d2d(19, AVRH: avg rel hum from surface to the hgh where temp is freezing
50. d2d(20, : surface virtual temperature (Kelvin)
51. d2d(21, SCAP: Convective Available Pot Energy (CAPE) of surface parcel
52. d2d(22, SCIN: Convective Inhibition (CIN) of surface parcel (J/kg)
53. d2d(23, SLFC: Level of Free Convection (LFC) of surface parcel (m AGL)
54. d2d(24, SFEL: Equilibrium Level (EL) of surface parcel (m AGL)
55. d2d(25, SFLI: Lifted Index (LI) of surface parcel (degrees)
56. d2d(26, SEHI: Energy-Helicity Index (EHI) of surface parcel
57. d2d(27, SMPL: Maximum Parcel Level: level (m AGL) at which the negative
58. d2d(28, UCAP: same as 21, except for the most unstable parcel
59. d2d(29, UCIN: same as 28, except for CIN
60. d2d(30, ULFC: same as 28, except for LFC
61. d2d(31, UNEL: same as 28, except for EL
62. d2d(32, UNLI: same as 28, except for LI
63. d2d(33, UEHI: same as 28, except for EHI
64. d2d(34, UMPL: same as 27, except for most unstable parcel in lowest 300 mb
65. d2d(35, UHGT: height (m AGL) of the most unstable (highest theta-e) parcel
66. d2d(36, DDC1: downdraft CAPE (dCAPE) for a parcel 1 km AGL
67. d2d(37, DDC3: dCAPE for a parcel 3 km AGL
68. d2d(38, DDC0: dCAPE for the parcel at 0 Celsius
69. d2d(39, ACAP: same as 21, except for a parcel with average characteristics
70. d2d(40, ACIN: same as 39, except for CIN
71. d2d(41, ALFC: same as 39, except for LFC
72. d2d(42, AVEL: same as 39, except for EL
73. d2d(43, AVLI: same as 39, except for LI
74. d2d(44, AEHI: same as 39, except for EHI
75. d2d(45, AMPL: same as 27, except for the ”average” parcel
76. d2d(46, SRLO: magnitude of the storm-relative flow for the 0-2 km agl
77. d2d(47, SRMD: same as 46, except for the 4-6 km agl layer
78. d2d(48, SRHI: same as 46, except for the 9-11 km agl layer
79. d2d(49, SBRN: Bulk Richardson Number (BRN) calculated according to

80. d2d(50, BSHR: BRN shear. See Eq. 3.4.58 of Bluestein Vol. II.
81. d2d(51, UBRN: same as 49, except for the most unstable parcel.
82. d2d(52, DT75: temperature difference (C) between 700 and 500 mb.
83. d2d(53, LLSM: magnitude (kts) of the low-level shear vector (surface
84. d2d(54, VTOT: Vertical Totals Index (C)
85. d2d(55, CTOT: Cross Totals Index (C)
86. d2d(56, TTOT: Total Totals Index (C)
87. d2d(57, AM35: average wind speed in the 500-300 mb layer (knots)
88. d2d(58, MXTE: maximum theta-e (Kelvin) in the lowest 300 mb
89. d2d(59, MCNV: surface moisture convergence [(g/kg)/hr]
90. d2d(60, SSHR: wind speed at specified height minus surface wind speed (kts)
91. d2d(61, AVOR: mean absolute vorticity in a layer ($\times 10^5$)
92. d2d(62, LAPS: mean lapse rate in the 850-500 mb layer (C/km)
93. d2d(63, MSHR: mean shear through a specified depth (hodograph length over
94. d2d(65, WNDX: WINDEX parameter (max gust potential in knots)
95. d2d(66,06SM: 0-6 km shear magnitude (knots)
96. d2d(67,DLSM: deep-layer shear vector magnitude (knots). The upper vector
97. d2d(68, SLCL: surface parcel LCL (m agl).NOTE: I convert it from mb to magl
98. d2d(69, ALCL: average parcel LCL (m agl). See NOTE above.
99. d2d(70, ULCL: most unstable parcel LCL (m agl). See NOTE above.
100. d2d(71, SARH: average RH (percent) below the surface parcel's LCL
101. d2d(72, AARH: average RH (percent) below the average parcel's LCL
102. d2d(73, UARH: average RH (percent) below the most unstable parcel's LCL
103. d2d(74, SVGP: Vorticity Generation Potential (VGP) using surface-based CAPE
104. d2d(75, SCVT: convective temperature (F) of surface parcel
105. d2d(76, ACVT: same as 75, except for "average parcel"
106. d2d(77, PCPW: precipitable water in entire sounding (inches)
107. d2d(78, DD70: dew point depression at 700 mb (Kelvin)
108. d2d(79, DD50: dew point depression at 500 mb (Kelvin)
109. d2d(80, MXDD: maximum dew point depression in the layer 700-400 mb (Kelvin)
110. d2d(81, HMTE: height (m agl) of the minimum theta-e below 400 mb
111. d2d(82, DDCU: dCAPE for the parcel defined in d2d(81,
112. d2d(83, TEDF: surface theta-e minus minimum theta-e below 400 mb (K)
113. d2d(84, DDCL: dCAPE from the surface parcel LCL in d2d(68,
114. d2d(85, OMEG: RUC-II vertical velocity (omega; microbars/sec) at specified
115. d2d(86, AOML: average omega (vertical velocity; microbars/sec) in the low-
116. d2d(87, KIDX:: K-Index (C)
117. d2d(88, HLCY:: RUC-II Helicity (m2/s2)
118. d2d(89, CAPE:: RUC-II CAPE (J/kg)
119. d2d(90, CINS:: RUC-II CIN (J/kg)
120. d2d(91, LIFT:: RUC-II Lifted Index (C)
121. d2d(92, LFT4:: RUC-II Another Lifted Index (C)
122. d2d(93, USSI: Shear Stability Index (SSI; W. Martin) for MU parcel

123. d2d(94, SWIX:: Showalter Index for MU parcel (K)
124. d2d(95, SWET:: Severe Weather (SWEAT) Index
125. d2d(96, AMR1: Average Mixing Ratio in 0-1 km layer (g/kg)
126. d2d(97, AMR3: Average Mixing Ratio in 0-3 km layer (g/kg)
127. d2d(98, AMR6: Average Mixing Ratio in 0-6 km layer (g/kg)
128. d2d(99, SRH1: estimated 0-1 km storm relative helicity
129. d2d(100, SRH2: estimated 0-2 km storm relative helicity
130. d2d(101, ARH1: Average Relative Humidity in 0-1 km layer (%)
131. d2d(102, 01SM: 0-1 km shear magnitude (knots)
132. d2d(103, 03SM: 0-3 km shear magnitude (knots)
133. d2d(104, 27SM: 27% UNEL (corresp. to 0-3 km) shear magnitude (knots)
134. d2d(105, 55SM: 55% UNEL (corresp. to 0-6 km) shear magnitude (knots)
135. d2d(106, 18SR: 0-18% UNEL (corresp. to 0-2 km) storm-relative flow (knots)
136. d2d(107, 55SR: 36-55% UNEL (corresp. to 4-6 km) storm-relative flow (knots)
137. d2d(108, 82SR: 82-100% UNEL (corresp. to 9-11 km) storm-relative flow
138. d2d(109, ULMB: Level of Maximum Bouyancy (from most-unstable parcel)
139. d2d(110, UMXB: Maximum Bouyancy (from most-unstable parcel) (m2/s2)
140. d2d(111, MBSM: ULMB (corresp. to 0-6 km) shear magnitude (knots)
141. d2d(112, MBSR: 20% below ULMB (corresp. to 4-6 km) storm-relative flow
142. d2d(113, HODO: 0-6km Bulk Hodograph Curvature (=0 straight; > 0 cyc;
143. d2d(114, LLLR: Low-Level (ULFC to ULFC+1km) Lapse Rate (C/km)
144. d2d(115, SNCA: Normalized SCAP [divide by z(SFEL)-z(SLFC)]
145. d2d(116, UNCA: Normalized UCAP [divide by z(UNEL)-z(ULFC)]
146. d2d(117, ANCA: Normalized ACAP [divide by z(AVEL)-z(ALFC)]
147. d2d(118, UCA3: UCAP from ULFC to ULFC+3km
148. d2d(119, UNC3: UCAP from ULFC to ULFC+3km $\div$ UCAP (%age of total)
149. d2d(120, UCAB: UCAP from sfc to 3 km AGL
150. d2d(121, UNCB: UCAP from sfc to 3 km AGL divided by UCAP (%age of total)
151. d2d(122, SR20:: Storm-relative flow (knots) at H253 level(1km surrounding).
152. d2d(123, AMEL: Average wind speed (kts) in 100 mb layer surrounding UNEL.
153. d2d(124, AWB7: Average wet bulb temp (K) from sfc to 700 mb.
154. d2d(125, HWBZ: Height (m) of the level at which the wet-bulb temp = 273K.

TDA

1. TVS base (m) [0-8000]
2. TVS depth (m) [0-10000]
3. TVS low-level gate-to-gate velocity difference (m/s) [0-90]
4. TVS maximum gate-to-gate velocity difference (m/s) [0-90]
5. TVS height of maximum gate-to-gate velocity difference (m) [1-11000]
6. TVS low-level shear (m/s/km) [0-350]
7. TVS maximum shear (m/s/km) [0-350]

8. TVS height of maximum shear (m) [1-11000]
9. TVS Tornado Strength Index (TSI)
10. TVS Range (km) [0-150]
11. BWER Overall Confidence (0-100%)
12. d2d(1, : actual surface pressure (mb)
13. d2d(2, : number of upper-air pressure levels lying below ground
14. d2d(3, : surface u-component (north-relative ; m/s)
15. d2d(4, : surface v-component (north-relative ; m/s)
16. d2d(5, H253: height of the 253 K temperature surface (m
17. d2d(6, H273: height of the 273 K temperature surface (m
18. d2d(7, UAVE: average u-component over a specified depth (north-relative)
19. d2d(8, VAVE: average v-component over a specified depth (north- relative)
20. d2d(9, : average wind speed over a specified depth (m/s)
21. d2d(10, STSP: estimated storm speed (m/s)
22. d2d(11, : u-component of estimated storm motion vector(north-relative)
23. d2d(12, : v-component of estimated storm motion vector(north-relative)
24. d2d(13, : same as 7, , except for grid-relative. See
25. d2d(14, : same as 8, , except for grid-relative
26. d2d(15, : same as 11, , except for grid-relative
27. d2d(16, : same as 12, , except for grid-relative
28. d2d(17, SRH3: estimated 0-3 km storm relative helicity
29. d2d(18, SFRH: surface relative humidity (percent)
30. d2d(19, AVRH: avg rel hum from surface to the hgh
31. d2d(20, : surface virtual temperature (Kelvin)
32. d2d(21, SCAP: Convective Available Pot Energy (CAPE) of surface parcel
33. d2d(22, SCIN: Convective Inhibition (CIN) of surface parcel (J/kg)
34. d2d(23, SLFC: Level of Free Convection (LFC) of surface parcel
35. d2d(24, SFEL: Equilibrium Level (EL) of surface parcel (m AGL)
36. d2d(25, SFLI: Lifted Index (LI) of surface parcel (degrees)
37. d2d(26, SEHI: Energy-Helicity Index (EHI) of surface parcel
38. d2d(27, SMPL: Maximum Parcel Level: level (m AGL) at which
39. d2d(28, UCAP: same as 21, except for the most unstable
40. d2d(29, UCIN: same as 28, except for CIN
41. d2d(30, ULFC: same as 28, except for LFC
42. d2d(31, UNEL: same as 28, except for EL
43. d2d(32, UNLI: same as 28, except for LI
44. d2d(33, UEHI: same as 28, except for EHI
45. d2d(34, UMPL: same as 27, except for most unstable parcel
46. d2d(35, UHGT: height (m AGL) of the most unstable (highest
47. d2d(36, DDC1: downdraft CAPE (dCAPE) for a parcel 1 km
48. d2d(37, DDC3: dCAPE for a parcel 3 km AGL
49. d2d(38, DDC0: dCAPE for the parcel at 0 Celsius
50. d2d(39, ACAP: same as 21, except for a parcel with

51. d2d(40, ACIN: same as 39, except for CIN
52. d2d(41, ALFC: same as 39, except for LFC
53. d2d(42, AVEL: same as 39, except for EL
54. d2d(43, AVLI: same as 39, except for LI
55. d2d(44, AEHI: same as 39, except for EHI
56. d2d(45, AMPL: same as 27, except for the "average" parcel
57. d2d(46, SRLO: magnitude of the storm-relative flow for the 0-2
58. d2d(47, SRMD: same as 46, except for the 4-6 km
59. d2d(48, SRHI: same as 46, except for the 9-11 km
60. d2d(49, SBRN: Bulk Richardson Number (BRN) calculated according to
61. d2d(50, BSHR: BRN shear. See Eq. 3.4.58 of Bluestein
62. d2d(51, UBRN: same as 49, except for the most unstable
63. d2d(52, DT75: temperature difference (C) between 700 and 500 mb.
64. d2d(53, LLSM: magnitude (kts) of the low-level shear vector (surface
65. d2d(54, VTOT: Vertical Totals Index (C)
66. d2d(55, CTOT: Cross Totals Index (C)
67. d2d(56, TTOT: Total Totals Index (C)
68. d2d(57, AM35: average wind speed in the 500-300 mb layer
69. d2d(58, MXTE: maximum theta-e (Kelvin) in the lowest 300 mb
70. d2d(59, MCNV: surface moisture convergence [(g/kg)/hr]
71. d2d(60, SSHR: wind speed at specified height minus surface wind
72. d2d(61, AVOR: mean absolute vorticity in a layer ($\times 10^5$)
73. d2d(62, LAPS: mean lapse rate in the 850-500 mb layer
74. d2d(63, MSHR: mean shear through a specified depth (hodograph length
75. d2d(65, WNDX: WINDEX parameter (max gust potential in knots)
76. d2d(66,06SM: 0-6 km shear magnitude (knots)
77. d2d(67,DLSM: deep-layer shear vector magnitude (knots). The upper vector is
78. d2d(68, SLCL: surface parcel LCL (m agl).NOTE: I convert it
79. d2d(69, ALCL: average parcel LCL (m agl). See NOTE above.
80. d2d(70, ULCL: most unstable parcel LCL (m agl). See NOTE
81. d2d(71, SARH: average RH (percent) below the surface parcel's LCL
82. d2d(72, AARH: average RH (percent) below the average parcel's LCL
83. d2d(73, UARH: average RH (percent) below the most unstable parcel's
84. d2d(74, SVGP: Vorticity Generation Potential (VGP) using surface-based CAPE
85. d2d(75, SCVT: convective temperature (F) of surface parcel
86. d2d(76, ACVT: same as 75, except for "average parcel"
87. d2d(77, PCPW: precipitable water in entire sounding (inches)
88. d2d(78, DD70: dew point depression at 700 mb (Kelvin)
89. d2d(79, DD50: dew point depression at 500 mb (Kelvin)
90. d2d(80, MXDD: maximum dew point depression in the layer 700-400
91. d2d(81, HMTE: height (m agl) of the minimum theta-e below
92. d2d(82, DDCU: dCAPE for the parcel defined in d2d(81,
93. d2d(83, TEDF: surface theta-e minus minimum theta-e below 400 mb

94. d2d(84, DDCL: dCAPE from the surface parcel LCL in d2d(68,
95. d2d(85, OMEG: RUC-II vertical velocity (omega; microbars/sec) at a specified
96. d2d(86, AOML: average omega (vertical velocity; microbars/sec) in the low-
97. d2d(87, KIDX:: K-Index (C)
98. d2d(88, HLCY:: RUC-II Helicity (m2/s2)
99. d2d(89, CAPE:: RUC-II CAPE (J/kg)
100. d2d(90, CINS:: RUC-II CIN (J/kg)
101. d2d(91, LIFT:: RUC-II Lifted Index (C)
102. d2d(92, LFT4:: RUC-II Another Lifted Index (C)
103. d2d(93, USSI: Shear Stability Index (SSI; W. Martin) for MU
104. d2d(94, SWIX:: Showalter Index for MU parcel (K)
105. d2d(95, SWET:: Severe Weather (SWEAT) Index
106. d2d(96, AMR1: Average Mixing Ratio in 0-1 km layer (g/kg)
107. d2d(97, AMR3: Average Mixing Ratio in 0-3 km layer (g/kg)
108. d2d(98, AMR6: Average Mixing Ratio in 0-6 km layer (g/kg)
109. d2d(99, SRH1: estimated 0-1 km storm relative helicity
110. d2d(100, SRH2: estimated 0-2 km storm relative helicity
111. d2d(101, ARH1: Average Relative Humidity in 0-1 km layer (%)
112. d2d(102, 01SM: 0-1 km shear magnitude (knots)
113. d2d(103, 03SM: 0-3 km shear magnitude (knots)
114. d2d(104, 27SM: 27% UNEL (corresp. to 0-3 km) shear magnitude
115. d2d(105, 55SM: 55% UNEL (corresp. to 0-6 km) shear magnitude
116. d2d(106, 18SR: 0-18% UNEL (corresp. to 0-2 km) storm-relative flow
117. d2d(107, 55SR: 36-55% UNEL (corresp. to 4-6 km) storm-relative flow
118. d2d(108, 82SR: 82-100% UNEL (corresp. to 9-11 km) storm-relative flow
119. d2d(109, ULMB: Level of Maximum Bouyancy (from most-unstable parcel) (m
120. d2d(110, UMXB: Maximum Bouyancy (from most-unstable parcel) (m2/s2)
121. d2d(111, MBSM: ULMB (corresp. to 0-6 km) shear magnitude (knots)
122. d2d(112, MBSR: 20% below ULMB (corresp. to 4-6 km) storm-relative
123. d2d(113, HODO: 0-6km Bulk Hodograph Curvature (=0 straight; > 0 cyc;
124. d2d(114, LLLR: Low-Level (ULFC to ULFC+1km) Lapse Rate (C/km)
125. d2d(115, SNCA: Normalized SCAP [divide by z(SFEL)-z(SLFC)]
126. d2d(116, UNCA: Normalized UCAP [divide by z(UNEL)-z(ULFC)]
127. d2d(117, ANCA: Normalized ACAP [divide by z(AVEL)-z(ALFC)]
128. d2d(118, UCA3: UCAP from ULFC to ULFC+3km
129. d2d(119, UNC3: UCAP from ULFC to ULFC+3km divided by UCAP
130. d2d(120, UCAB: UCAP from sfc to 3 km AGL
131. d2d(121, UNCB: UCAP from sfc to 3 km AGL divided
132. d2d(122, SR20:: Storm-relative flow (knots) at H253 level (1km surrounding).
133. d2d(123, AMEL: Average wind speed (kts) in 100 mb layer
134. d2d(124, AWB7: Average wet bulb temp (K) from sfc to
135. d2d(125, HWBZ: Height (m) of the level at which the

6 Appendix B

This appendix lists the pair of variables in MDA and TDA with class-conditional linear correlation coefficients, r_0 and r_1, larger than 0.9. Such pair of variables may be considered (statistically) equivalent.

MDA pair	r	r_0	r_1	TDA pair	r	r_0	r_1
(21,29)	0.91	0.90	0.94	(5,8)	0.97	0.97	0.96
(25,29)	0.96	0.96	0.97	(6,7)	0.94	0.94	0.90
(31,32)	-0.96	-0.96	-0.97	(12,13)	-0.97	-0.97	-0.97
(37,43)	0.97	0.97	0.95	(18,24)	0.98	0.98	0.95
(37,45)	0.94	0.95	0.91	(19,23)	0.94	0.94	0.98
(38,42)	0.95	0.95	0.98	(19,25)	0.97	0.97	0.97
(38,44)	0.97	0.97	0.97	(19,27)	0.95	0.95	0.97
(38,46)	0.95	0.95	0.96	(20,21)	1.00	1.00	1.00
(39,40)	1.00	1.00	1.00	(22,26)	0.98	0.98	0.95
(41,45)	0.97	0.97	0.95	(23,27)	0.97	0.97	0.97
(42,46)	0.97	0.96	0.97	(24,26)	0.95	0.95	0.91
(43,45)	0.94	0.94	0.92	(25,27)	0.93	0.92	0.97
(44,46)	0.93	0.93	0.96	(28,98)	0.91	0.91	0.91
(47,117)	0.91	0.91	0.93	(28,109)	0.95	0.95	0.94
(47,128)	0.95	0.95	0.94	(29,78)	-0.98	-0.98	-0.98
(48,97)	-0.97	-0.97	-0.98	(35,38)	0.99	0.99	0.99
(54,57)	0.99	0.99	0.99	(36,101)	1.00	1.00	0.99
(55,120)	1.00	1.00	0.99	(39,99)	0.98	0.98	0.98
(58,118)	0.96	0.96	0.98	(39,120)	0.96	0.96	0.95
(58,139)	0.95	0.95	0.96	(43,102)	0.97	0.97	0.97
(62,121)	0.97	0.97	0.97	(47,82)	-0.93	-0.93	-0.90
(66,130)	-0.92	-0.92	-0.90	(47,111)	-0.93	-0.93	-0.91
(67,68)	0.92	0.92	0.92	(48,49)	0.93	0.93	0.92
(72,75)	0.94	0.94	0.97	(53,56)	0.96	0.96	0.97
(78,96)	0.94	0.94	0.94	(59,77)	0.95	0.95	0.94
(83,131)	1.00	1.00	1.00	(64,112)	1.00	1.00	1.00
(83,133)	0.97	0.97	0.96	(64,114)	0.97	0.97	0.96
(84,92)	-0.97	-0.97	-0.98	(65,73)	-0.98	-0.98	-0.98
(98,100)	-0.93	-0.93	-0.95	(79,81)	-0.94	-0.94	-0.95
(98,101)	-0.96	-0.96	-0.97	(79,82)	-0.96	-0.96	-0.98
(98,130)	-0.97	-0.97	-0.98	(79,111)	-0.97	-0.97	-0.99
(100,101)	0.97	0.97	0.98	(81,82)	0.97	0.97	0.98
(100,130)	0.95	0.95	0.95	(81,111)	0.96	0.96	0.96
(101,130)	0.98	0.99	0.98	(82,111)	0.99	0.99	0.98
(104,105)	0.95	0.95	0.94	(85,86)	0.95	0.95	0.94
(106,126)	0.95	0.95	0.94	(87,107)	0.94	0.94	0.94
(106,127)	0.99	0.99	0.99	(87,108)	0.99	0.99	0.99
(106,154)	0.92	0.92	0.93	(87,135)	0.91	0.91	0.92
(126,127)	0.97	0.97	0.97	(99,120)	0.93	0.93	0.93
(127,154)	0.92	0.92	0.91	(107,108)	0.96	0.96	0.97
(131,133)	0.97	0.97	0.96	(112,114)	0.97	0.97	0.96
(132,134)	0.92	0.92	0.94	(113,115)	0.94	0.94	0.95

7 Appendix C

This appendix contains figures that display the predcitive strength of every variable in MDA and in TDA, according to three measures of performance, and for 4 different storm types.

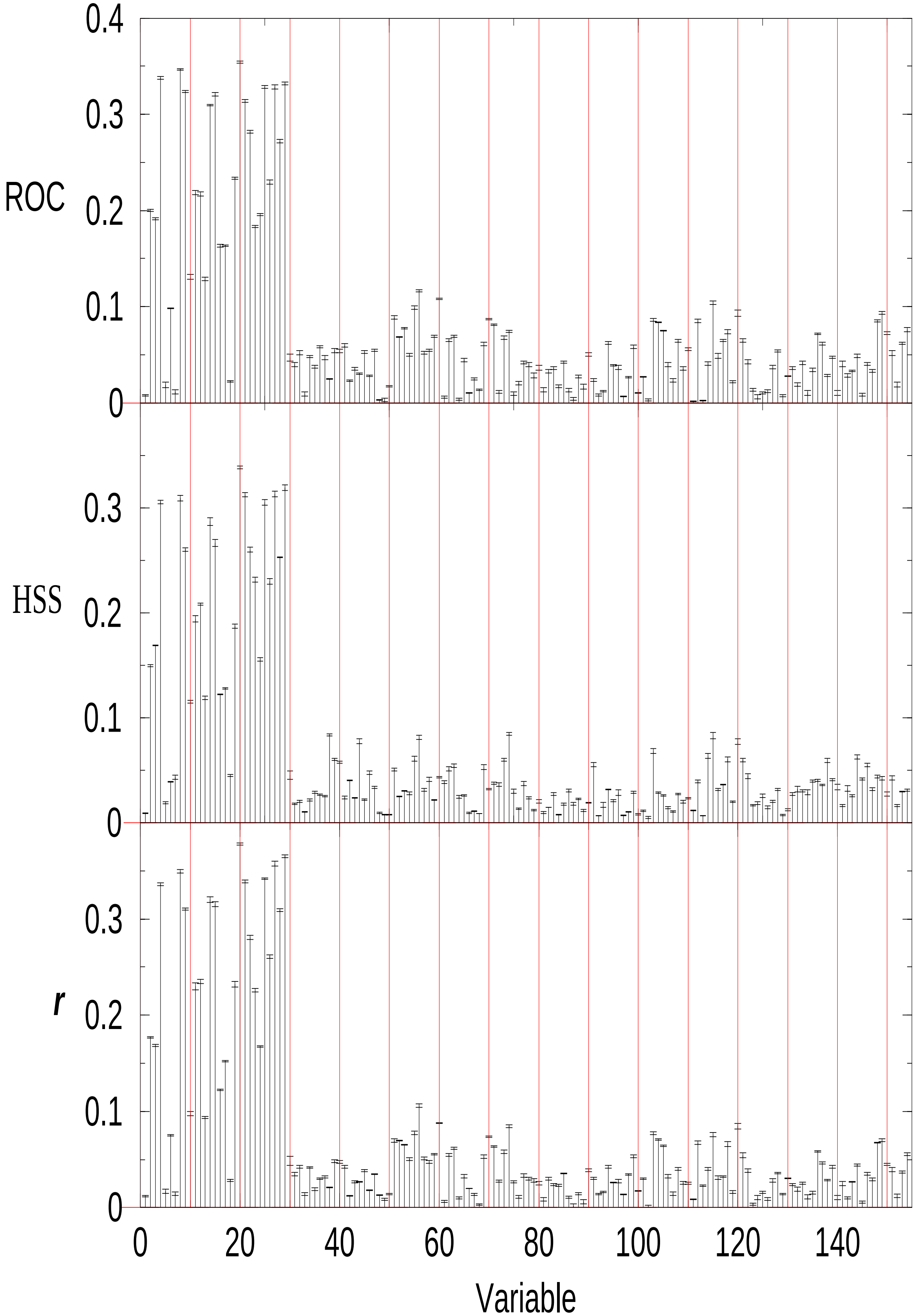

Figure 8: Predictive stength of MDA variables for isolated storms.

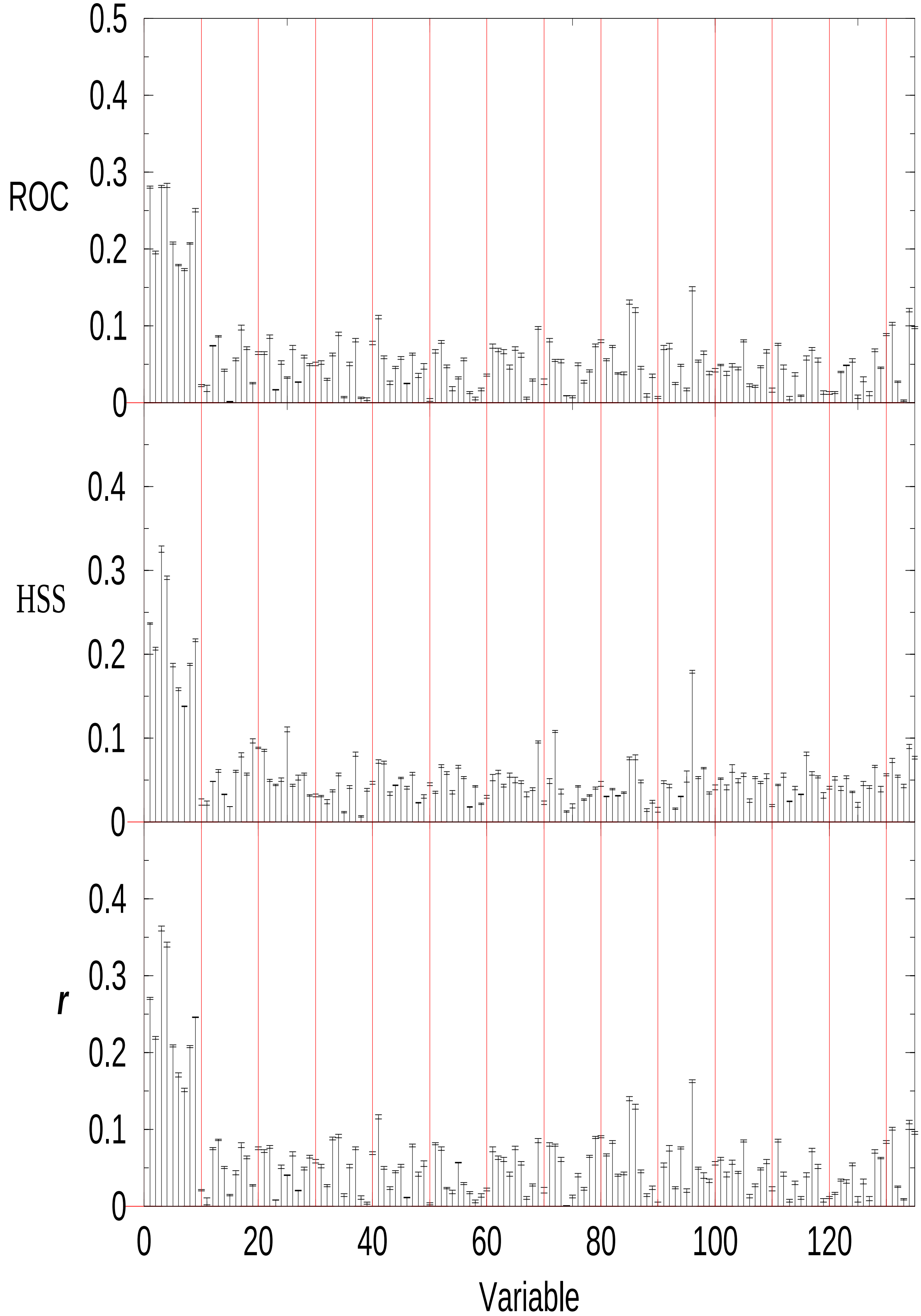

Figure 9: Predictive stength of TDA variables for isolated storms.

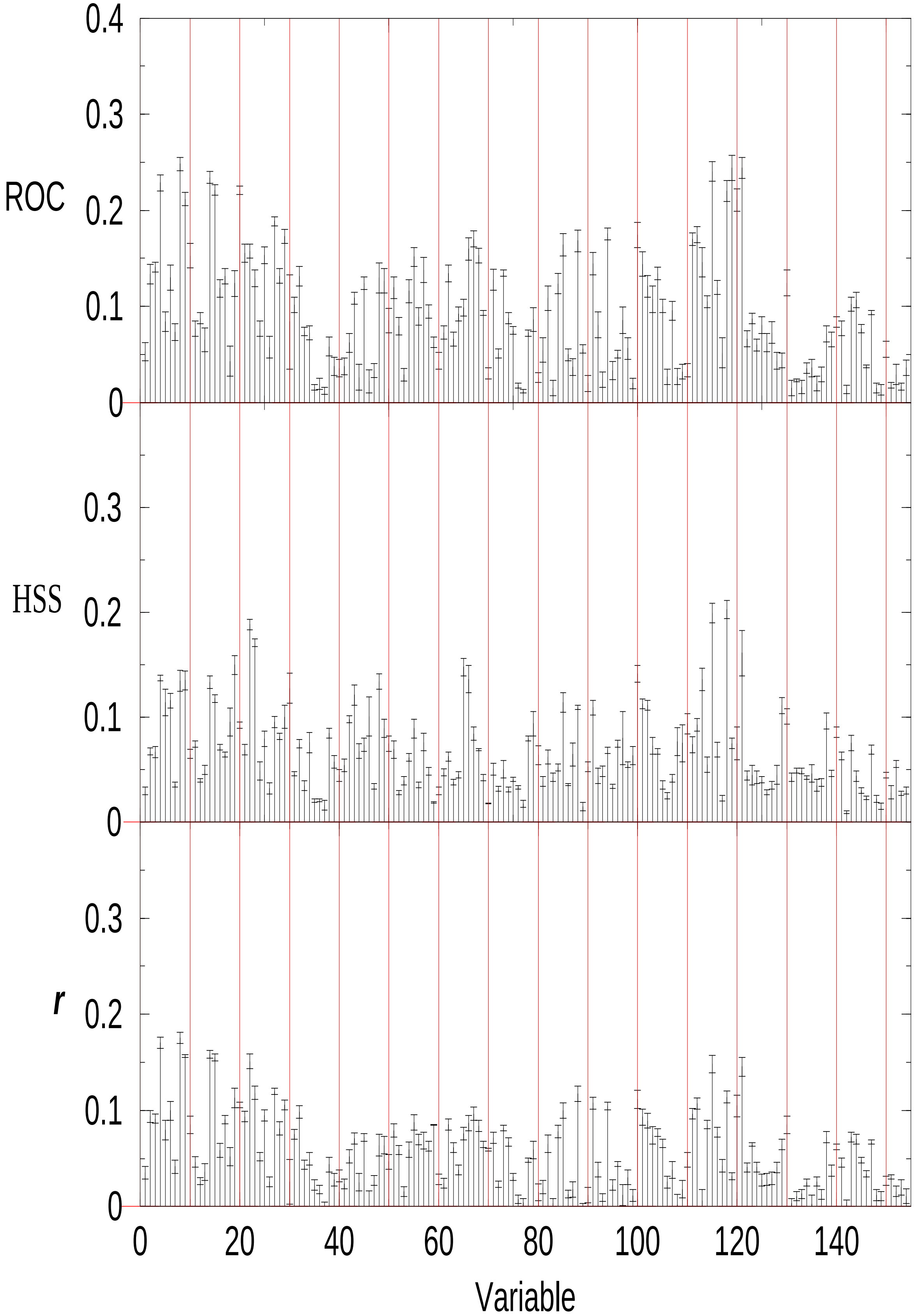

Figure 10: Predictive stength of MDA variables for mini supercell storms.

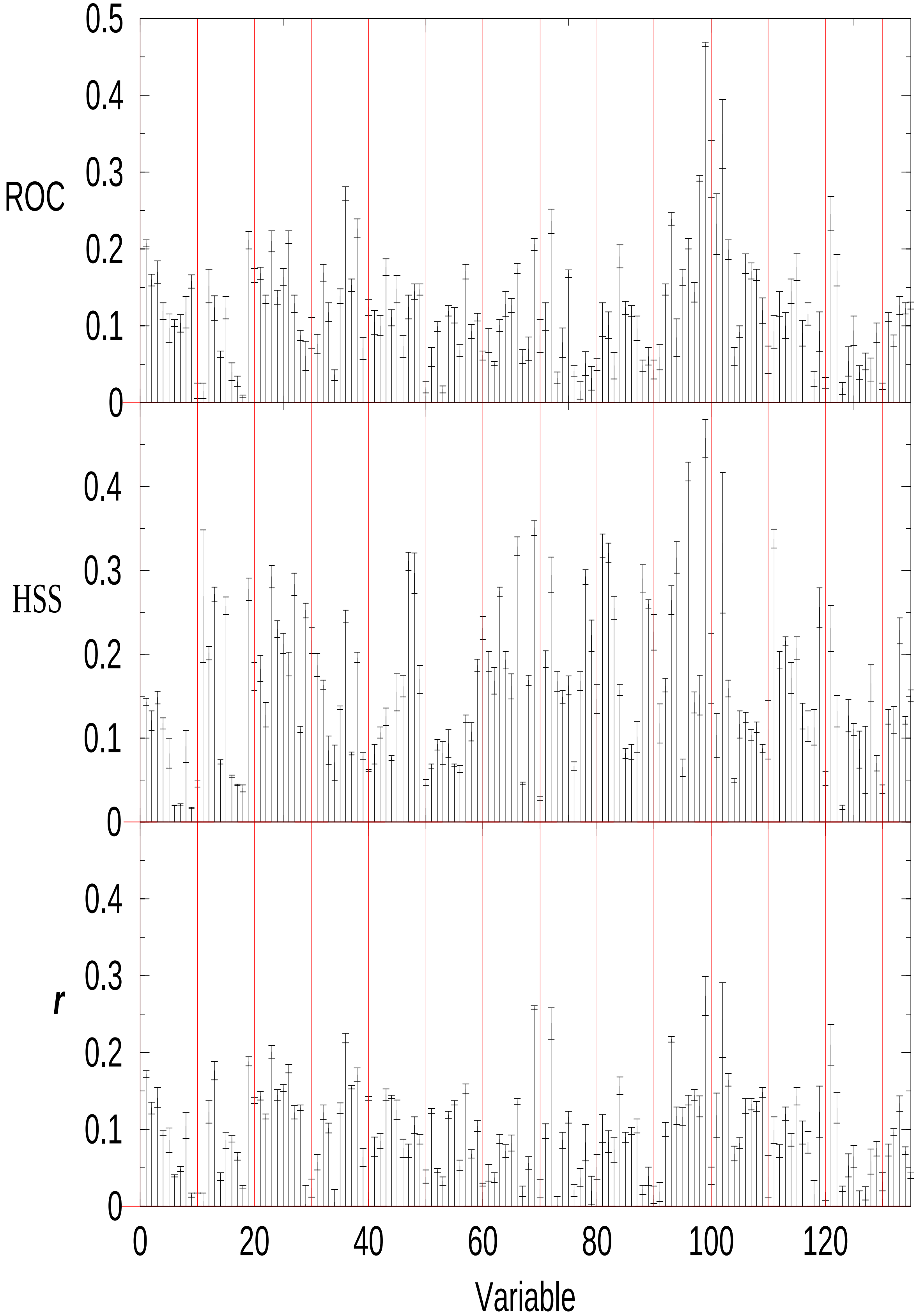

Figure 11: Predictive stength of TDA variables for mini supercell storms.

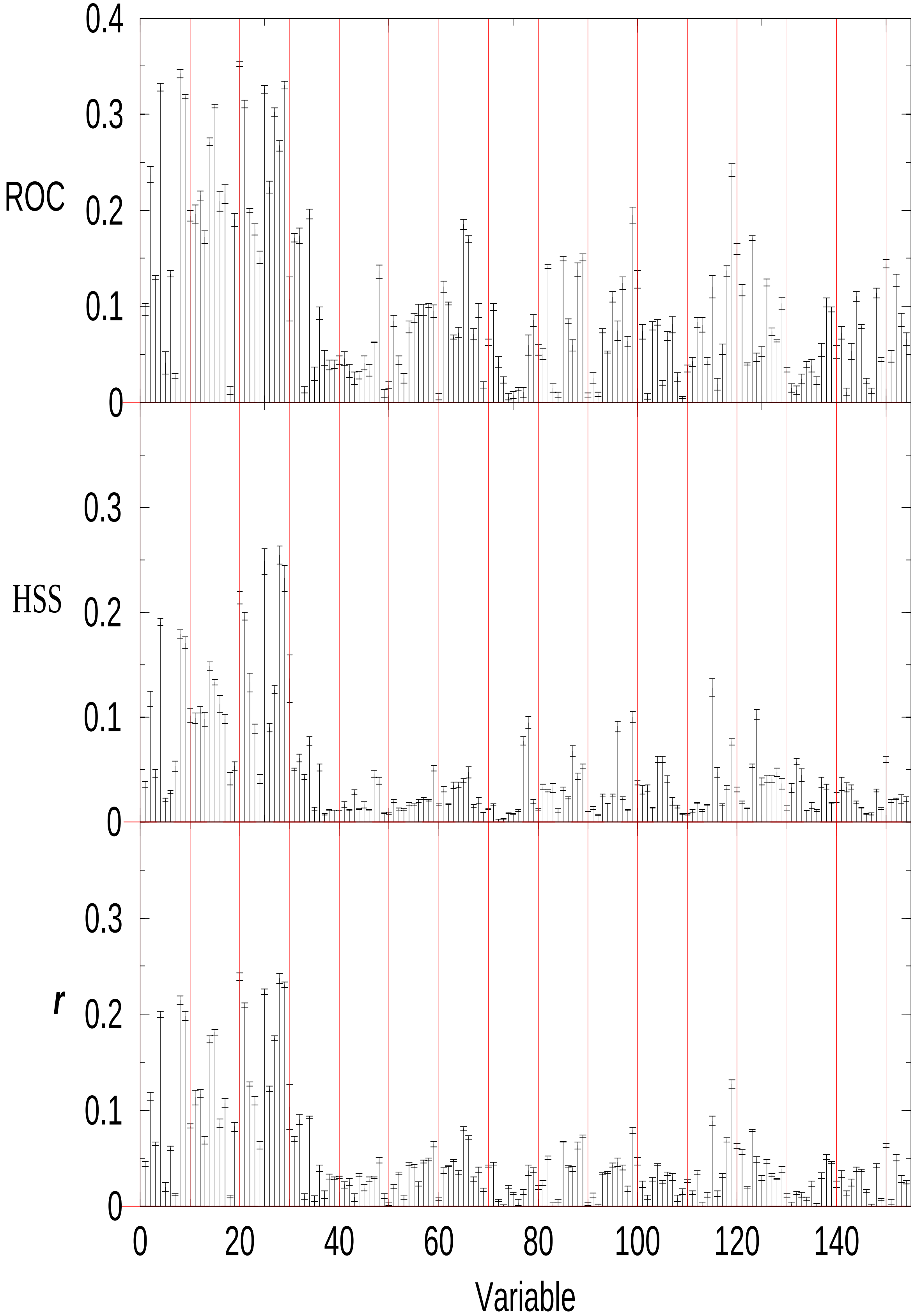

Figure 12: Predictive stength of MDA variables for squall line storms.

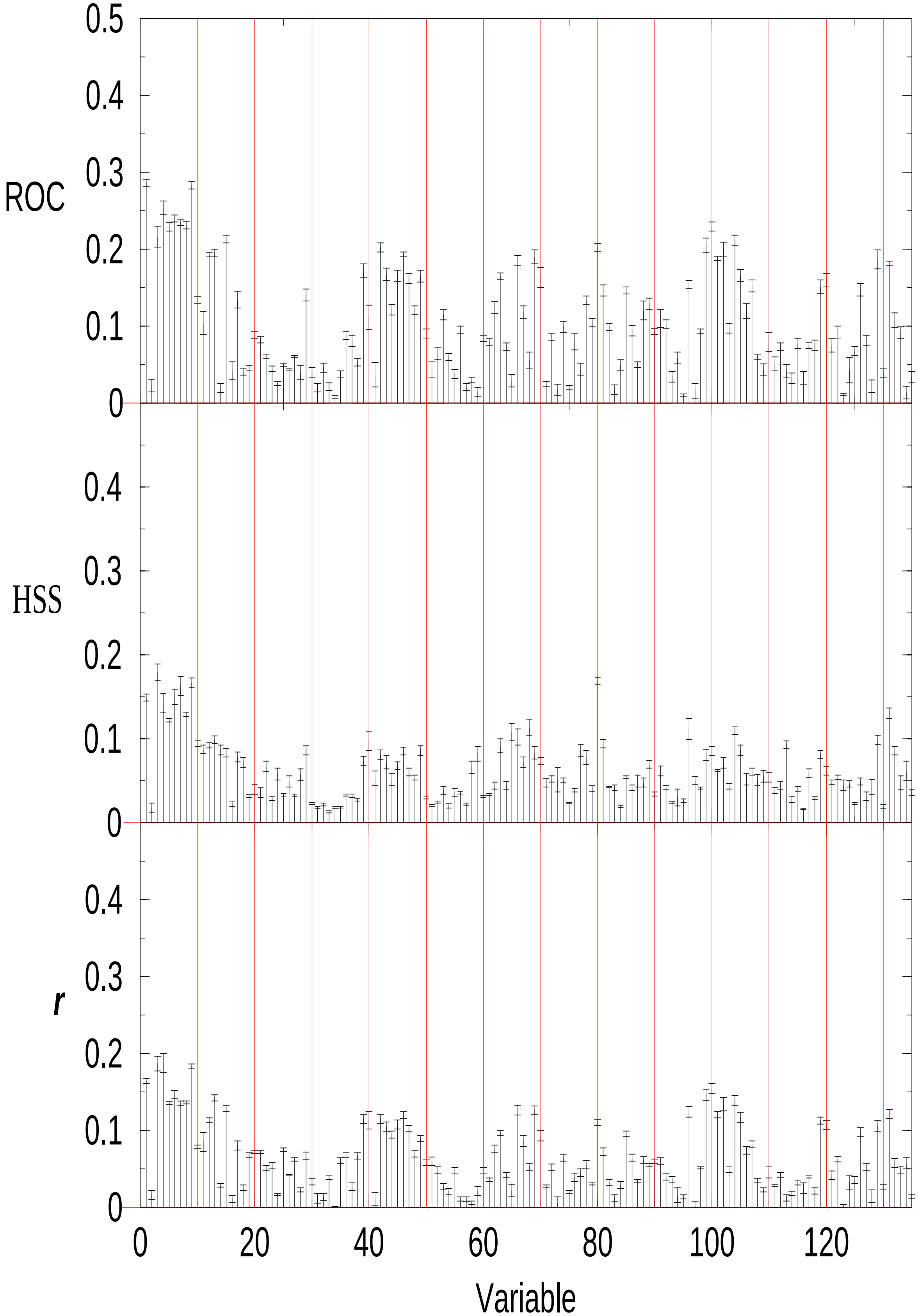

Figure 13: Predictive stength of TDA variables for squall line storms.

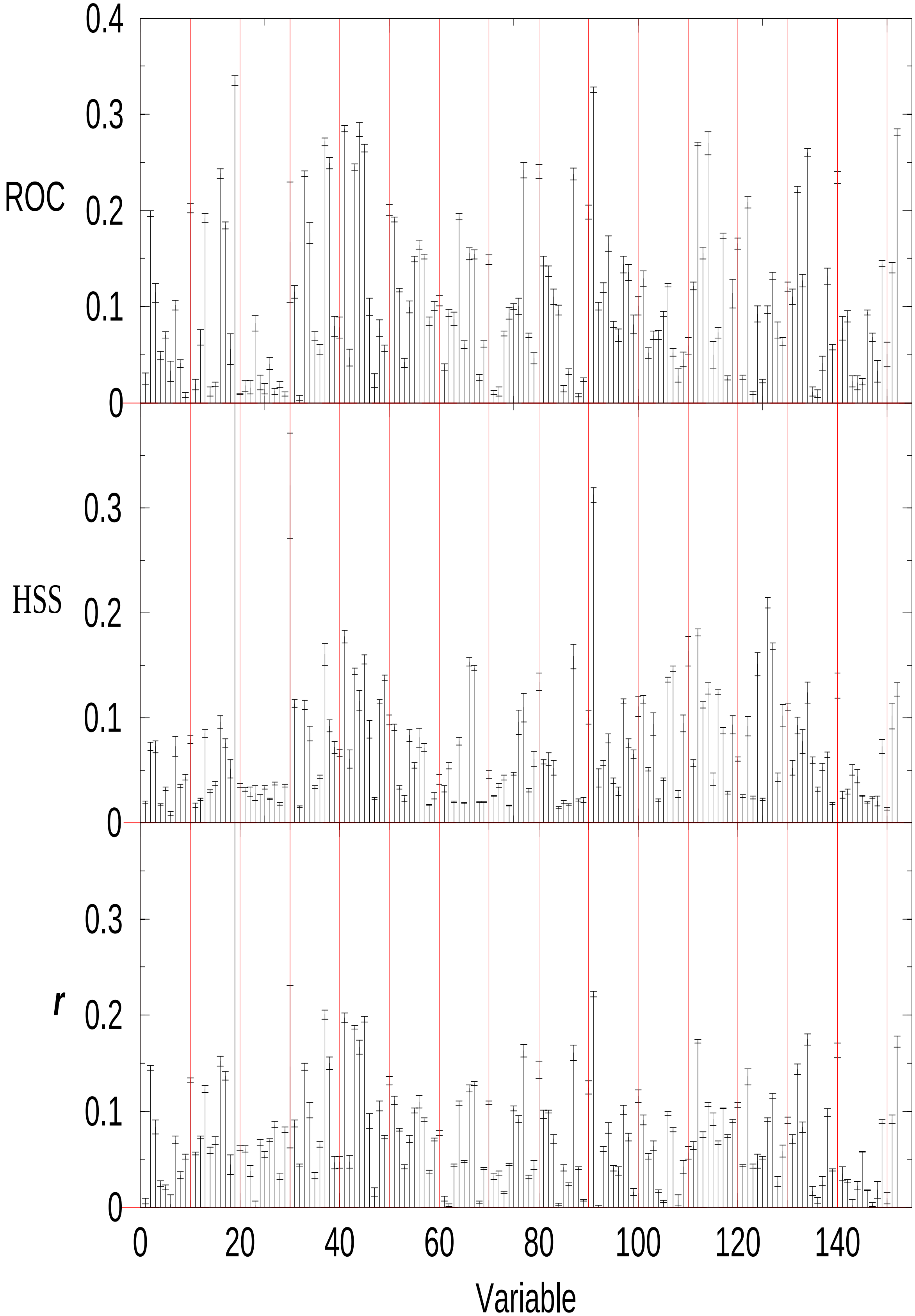

Figure 14: Predictive stength of MDA variables for tropical storms.

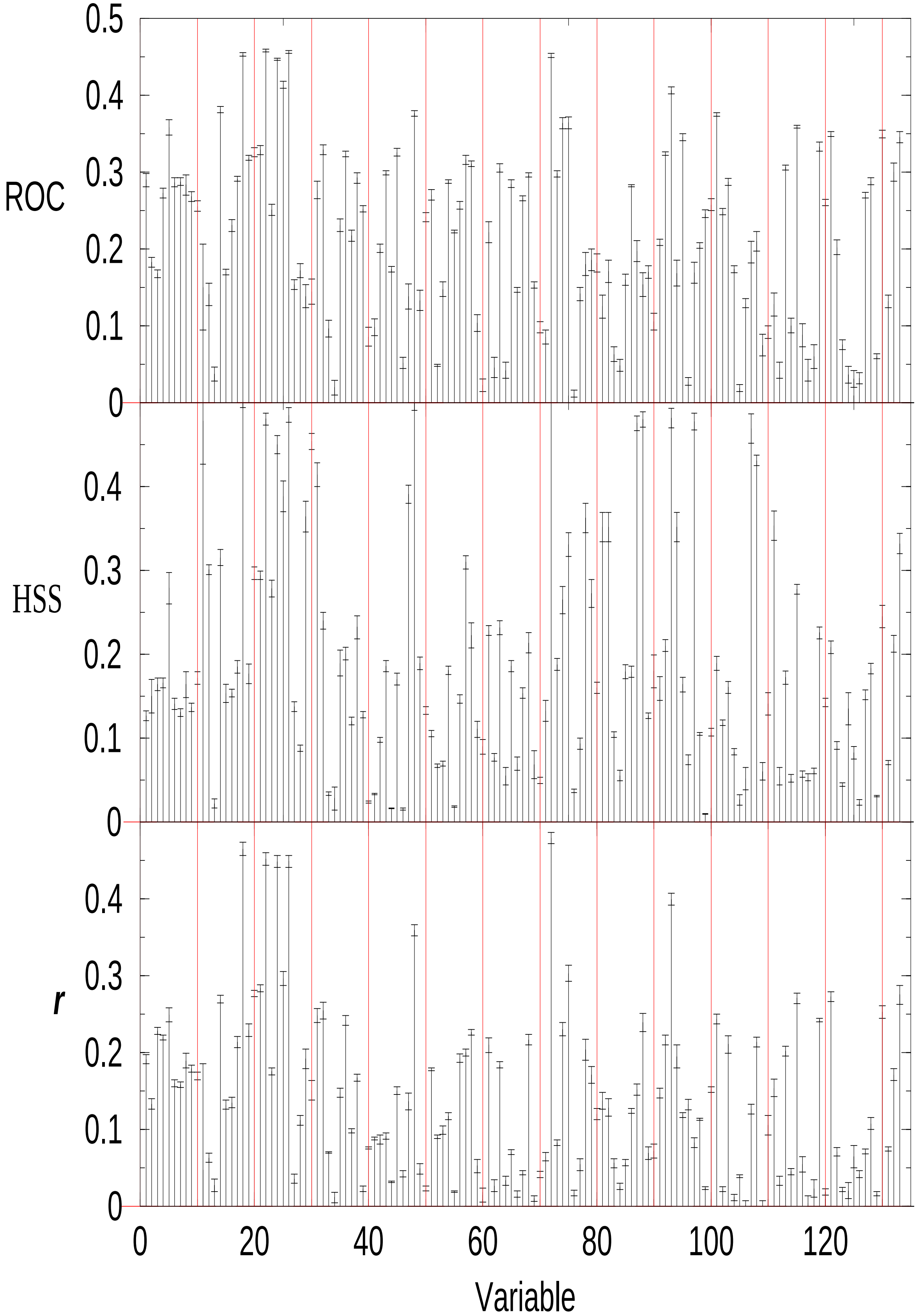

Figure 15: Predictive stength of TDA variables for tropical storms.

8 References

1. Marzban, C., 1998: Bayesian probability and scalar performance measures in Gaussian Models. *Journal of Applied Meteorology*, **37**, 72.

2. Marzban, C., E.D. Mitchell, and G. J. Stumpf, 1999: The Notion of "Best Predictors:" An Application to Tornado Diagnosis. *Wea. Forecasting*,**14** , 1007-1016.

3. Marzban, C., 2000: Neural Networks for Tornado Diagnosis. *Neural Computing and Applications*,**9 (2)**, 133-141.